Journal of Nanoparticle Research **2:** 123–131, 2000.

Invited paper

Dynamic light scattering measurement of nanometer particles in liquids

R. Pecora
Department of Chemistry, Stanford University, Stanford, CA 94305-5080, USA (E-mail: pecora@stanford.edu)

Received 15 January 2000; accepted in revised form 14 June 2000

Key words: nanoparticle, characterization, light scattering, PCS, interferometry, diffusion, polydispersivity

Abstract

Dynamic light scattering (DLS) techniques for studying sizes and shapes of nanoparticles in liquids are reviewed. In photon correlation spectroscopy (PCS), the time fluctuations in the intensity of light scattered by the particle dispersion are monitored. For dilute dispersions of spherical nanoparticles, the decay rate of the time autocorrelation function of these intensity fluctuations is used to directly measure the particle translational diffusion coefficient, which is in turn related to the particle hydrodynamic radius. For a spherical particle, the hydrodynamic radius is essentially the same as the geometric particle radius (including any possible solvation layers). PCS is one of the most commonly used methods for measuring radii of submicron size particles in liquid dispersions. Depolarized Fabry-Perot interferometry (FPI) is a less common dynamic light scattering technique that is applicable to optically anisotropic nanoparticles. In FPI the frequency broadening of laser light scattered by the particles is analyzed. This broadening is proportional to the particle rotational diffusion coefficient, which is in turn related to the particle dimensions. The translational diffusion coefficient measured by PCS and the rotational diffusion coefficient measured by depolarized FPI may be combined to obtain the dimensions of non-spherical particles. DLS studies of liquid dispersions of nanometer-sized oligonucleotides in a water-based buffer are used as examples.

Introduction

Dynamic light scattering (DLS) is the most versatile and useful set of techniques for measuring *in situ* the sizes, size distributions, and (in some cases) the shapes of nanoparticles in liquids (Berne & Pecora, 2000; Chu, 1991; Brown, 1993; Pecora, 1985; Schmitz, 1990). DLS, which has many variations, does not by itself identify the chemical nature of a nanoparticle. This demanding task requires information on sample history or, in the most general case, on species specific sensors (Vo-Dinh, 2000). Important competing techniques include drying the sample and using imaging methods such as electron microscopy. Drying the sample, however, and/or placing it on or near a surface can cause changes in the system that may not accurately reflect the nature of the species in the liquid dispersion. Other solution sizing techniques applicable to sizing nanoparticles in liquids include static scattering of radiation whose wavelength is comparable to the size of the particle. For nanoparticles, this includes mainly small angle X-ray and neutron scattering (Chu & Liu, 2000). DLS techniques are 'hydrodynamic' techniques in that they directly measure hydrodynamic quantities, usually the translational and/or rotational diffusion coefficients, which are then related to sizes and shapes via theoretical relations. Other hydrodynamic techniques applicable to nanoparticles in liquids include Raman correlation spectroscopy (Schrof et al., 1998), fluorescence correlation spectroscopy (Aragon & Pecora, 1975; Schrof et al., 1998; Startchev et al., 1998), fluorescence depolarization decay (Lakowicz, 1983), fluorescence recovery after photobleaching (Bu et al., 1994), forced Rayleigh scattering (also called holographic grating spectroscopy) (Graf et al., 2000) and various

birefringence techniques, such as transient electric birefringence decay (Eden & Elias, 1983) and the dynamic optical Kerr effect (Righini, 1993). We limit ourselves here to discussing DLS techniques – mainly photon correlation spectroscopy (PCS) and depolarized Fabry-Perot interferometry (FPI) and their application to the study of nanoparticles – defined here as particles with characteristic sizes from about 1 to about 50 nm – dispersed in liquids.

Photon correlation spectroscopy

PCS is now a standard technique that is widely utilized in biophysics, colloid and polymer laboratories. It may be used for routine particle characterization as well as for studies of the nature of interactions of molecules and particles in liquid dispersions. Commercial apparatus is available from several instrument companies.

PCS is based on fact that the intensity of light scattered from a dispersion of particles into a given scattering angle is the result of interference on the surface of a square-law detector between light scattered from different particles in the medium. The phases at the detector of the light scattered from different particles depend on the relative positions of the particles relative to the direction of the incoming and scattered light beams. Thus, at a given instant the total scattered intensity at a given scattering angle depends on the positions of the particles (structure). The particles, however, are constantly executing Brownian motion so that their positions fluctuate. Thus, the scattered intensity also fluctuates. These scattered intensity fluctuations occur on the time scale that it takes a particle to move a significant fraction of the wavelength of light.

The scattered intensity itself is a stochastic signal, since it reflects the thermal (Brownian) motion of the particles. To extract useful information from the signal, its time correlation function is computed. This is usually done using an autocorrelator – a computer equipped with special boards to allow rapid real-time calculation of the scattered intensity time correlation function.

A schematic of a PCS apparatus is shown in Figure 1. Light from a laser is focused on a sample and the light scattered at a given scattering angle is collected by a square law detector – a photomultiplier as shown in the figure or, as is becoming more common, an avalanche photodiode (Kaszuba, 1999). The output of the photomultiplier is then digitized by a photon counting system

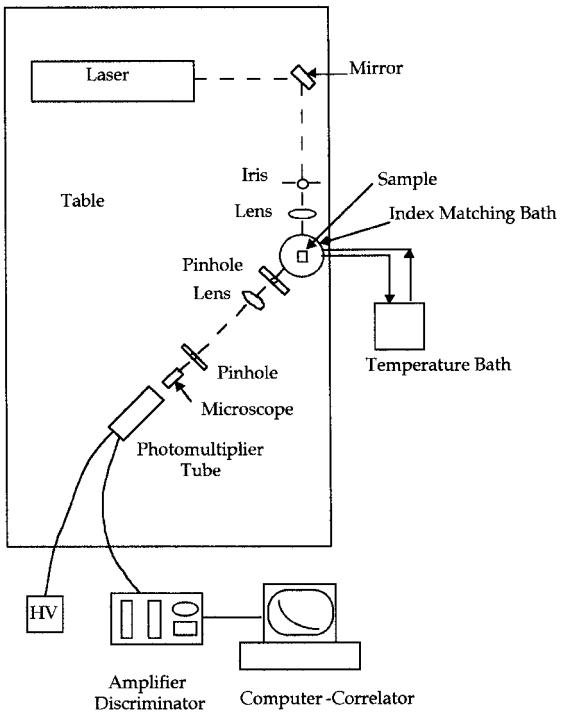

Figure 1. Schematic diagram of a PCS apparatus.

and the output sent to an autocorrelator. A modern PCS apparatus often utilizes fiber optics guides to both deliver the light to the sample and collect the scattered light and bring it to the detector. In fact, fiber optic guidance is essential in applying this technique to strongly scattering systems (Wiese & Horn, 1991).

This technique and its variants are also known by several other names. Among them are quasi-elastic light scattering, intensity fluctuation spectroscopy, optical (light) beating spectroscopy, and homodyne (or heterodyne) spectroscopy. DLS and PCS are, however, now the most common, although as mentioned above DLS (as well as quasi-elastic light scattering) is a more general term and also includes usually other techniques (such as FPI).

The normalized scattered intensity time autocorrelation function of the scattered light intensity may be written as

$$C(t) \equiv \frac{\langle I(t)I(0)\rangle}{\langle I(0)I(0)\rangle} = \left[1 + \gamma[g^{(1)}(t)]^2\right] \qquad (1)$$

where γ is a constant determined by the specific experimental setup and $g^{(1)}(t)$ is the normalized first order (scattered electric field) time autocorrelation function.

Note that this function appears squared in Eq. (1). In an ideal apparatus, the constant γ, often called the 'coherence factor,' is equal to 1, so that, in such a case, the normalized intensity autocorrelation function starts at a value of 2 at zero time delay and eventually decays to 1. In practice γ is usually < 1.

It may be shown for a dilute solution of monodisperse nanoparticles that $g^{(1)}(t)$ is a single exponential whose time decay is determined by the translational self-diffusion coefficient of the particle D and the length of the scattering vector q:

$$g^{(1)}(t) = \exp(-q^2 Dt) \tag{2}$$

The scattering vector length depends on the scattering angle θ, and the wavelength λ of the light in the scattering medium:

$$q = (4\pi/\lambda)\sin(\theta/2) \tag{3}$$

As may be seen from Eqs. (2) and (3), PCS, in this case, directly gives the translational self-diffusion coefficient of the nanoparticle. Although in principle, a measurement at only one scattering angle is necessary to obtain D, measurements are usually done at a series of scattering angles and the decay constant of $g^{(1)}(t)$ is plotted versus q^2. A straight line with a slope equal to D should be obtained.

For spherical particles in a dilute dispersion, the Stokes–Einstein relation relates the translational self-diffusion coefficient to the particle radius R

$$D = k_B T/6\pi\eta R \tag{4}$$

where k_B is Boltzmann's constant, T the absolute temperature and η is the viscosity of the suspending medium. Thus, for spherical nanoparticles the particle radius (including any solvation layer) may be derived from the PCS experiment.

In the more general case in which the particles are non-spherical or flexible, the radius derived from the self-diffusion coefficient and the Stokes–Einstein relation is called the 'hydrodynamic radius'. The hydrodynamic radius for non-spherical molecules is, of course, not equal to a geometrical particle 'radius'. The relation between the translational diffusion coefficient or hydrodynamic radius and the actual dimensions of non-spherical particles depends on the particle shape. We discuss this case further below in the section on FPI.

One of the difficulties in applying PCS to nanoparticles is that the scattered light signals are relatively weak in dilute solutions and the time scales are usually fast (smaller particles move faster). Thus, relatively intense (of the order of a 100 mW or more) laser sources are required to obtain acceptable signal to noise ratios in these experiments. Recently, the use of avalanche diodes as detectors instead of photomultiplier tubes has made it possible to perform PCS experiments with lower power lasers (Kaszuba, 1999). Lower power lasers are relatively cheap, easy to operate and transport and lessen the danger of appreciably heating the sample.

Polydispersity

Nanoparticle dispersions are often polydisperse; that is, there may be particles with a distribution of sizes and shapes rather than particles of a single size and shape. The particles in the distribution thus, in general, have different translational self-diffusion coefficients.

For a dilute solution, we may view the particles with a given diffusion coefficient (denoted by i) as contributing its own exponential to the first order correlation function so that

$$g^{(1)}(t) = \sum_i A_i \exp(-\Gamma_i t) \tag{5}$$

where $\Gamma_i = q^2 D_i$ is the reciprocal decay time and A_i is a weighting factor proportional to the fraction of the scattered intensity contributed by this subset of particles.

Thus, the first order time correlation function is now a sum of exponentials. One technique for characterizing this sum of exponentials is the method of cumulants.

In the cumulants method, the logarithm of the normalized correlation function $g^{(1)}(t)$ is expanded as a power series in the time:

$$\ln[g^{(1)}(t)] = -K_1 t + (1/2)K_2 t^2 + \cdots . \tag{6}$$

The coefficients K_n are the cumulants. K_1, the first cumulant, is equal to the average of the reciprocal relaxation time $K_1 = \langle(\Gamma)\rangle$. The second cumulant K_2 is a measure of the dispersion of the reciprocal relaxation time around the average value. Note that if K_2 (and higher order cumulants) are 0, the first order correlation function is a single exponential. The cumulant method is simple and most commercial autocorrelators include a computer program for calculating the first few cumulants.

A more powerful method, which has become the standard in analyzing PCS data, uses mathematical

algorithms to perform an inverse Laplace transform on the data to obtain the distribution function of relaxation times. Take the continuous limit of the sum in Eq. (5).

$$g^{(1)}(t) = \int_0^\infty A(\Gamma) \exp(\Gamma t)\, \mathrm{d}\Gamma \tag{7}$$

where $A(\Gamma)\,\mathrm{d}\Gamma$ is the fraction of the correlation function decaying with reciprocal relaxation time between Γ and $\Gamma + \mathrm{d}\Gamma$. Note from Eq. (7) that $g^{(1)}(t)$ is the Laplace transform of $A(\Gamma)$.

To find $A(\Gamma)$ from measurements of $g^{(1)}(t)$, we must invert the Laplace transform. This is an ill-conditioned problem. It turns out that we cannot simply find the ILT by picking the $A(\Gamma)$ that gives the best least squares fit to data. Mathematical techniques for performing such transforms, known as regularization techniques, have been developed by mathematicians and applied to the analysis of PCS data by Provencher (Provencher, 1982). Provencher has implemented his technique in a program called 'CONTIN', which has, sometimes in modified form, become the method of choice for analyzing PCS data. Basically, this program finds the smoothest non-negative $A(\Gamma)$ consistent with the data and the noise in it.

Extensive testing of CONTIN and its variants has been done. The method gives good estimates for the widths and peaks of unimodal distributions when the data has good signal to noise. Tests have also shown that PCS with CONTIN analysis is capable of resolving peaks in $A(\Gamma)$ as long as the separation of the $A(\Gamma)$ peaks is about a factor of two or more and the areas under the peaks are not very different (Flamberg & Pecora, 1984). Thus, it is, with these limitations, possible to detect and study bimodal particle distributions by this method. The output of CONTIN is frequently expressed in hydrodynamic radius rather than Γ. In addition, in favorable circumstances, the weight distribution and number distribution of particles can be obtained.

Examples of nanoparticle size distributions obtained using PCS have recently been given by Kaszuba (1999).

Concentration effects

The application of PCS described above to measure sizes of nanoparticles in liquid dispersions depends on the validity of the Stokes–Einstein relation and its analogs for non-spherical particles. The dispersion is assumed to be so dilute that there are no correlations between the nanoparticles. In more concentrated solutions the diffusion coefficient measured is the cooperative diffusion coefficient, which in the limit of $q \to 0$ becomes the mutual diffusion coefficient (Pusey & Tough, 1985).

If the concentration is not very much higher than dilute, the measured diffusion coefficient measured by PCS may be expanded in a power series in the concentration around the self-diffusion coefficient at infinite dilution, D_0

$$D = D_0(1 + k_\mathrm{D} c + \cdots) \tag{8}$$

where k_D is a coefficient that is usually positive for small particles. Thus, the measured diffusion coefficient for particles that do not aggregate increases with concentration, at least initially. The infinite dilution self-diffusion coefficient D_0 is the quantity that is used in conjunction with Eq. (4) to obtain the particle radius. The coefficient k_D can be related to the thermodynamic solution second virial coefficient and the frictional virial coefficient (Berne & Pecora, 2000; Pusey & Tough, 1985). In any case, to be assured that the self-diffusion coefficient at infinite dilution is being measured, it is desirable to do PCS studies as a function of nanoparticle concentration and to extrapolate to infinite dilution.

Depolarized Fabry-Perot interferometry

The rotational diffusion of nanoparticles is usually too fast to be easily measured by PCS. The measurement of the rotational diffusion coefficient of a nanoparticle may, however, often be performed using depolarized FPI. FPI is a DLS technique that utilizes the fact that light that exhibits intensity fluctuations is composed of a corresponding range of frequencies (spectrum). Thus, the frequency distribution of the scattered light contains information about the dynamics of molecules comprising the scattering system. Depolarized FPI refers to the case in which the incoming laser beam polarization is perpendicular to the scattering plane (plane in which the incoming and scattered beams propagate) and a polarizer is used to select the component of the scattered beam in the scattering plane.

An FPI is a high resolution monochrometer that resolves the scattered light into its component

frequencies. It is used most often in the frequency change range from about 1 MHz to 10 GHz. For nanoparticles the lower part of this range is the most important and is applicable to particles with characteristic sizes below about 10 nm. One important caveat is that the rotational motion is manifested in the depolarized component of the scattered light. For this component to be appreciably different from zero, the molecules must be optically anisotropic, that is, its polarizability in a laboratory-fixed system must vary as the particle rotates. It should be noted that even spherical particles could, because of their internal structure, sometimes exhibit an optical anisotropy. In fact, optically anisotropic spheres have become an important tool in colloid science (Piazza & Gegiorgio, 1992; Piazza et al., 1989; Camins & Russo, 1994).

A schematic of the simplest form of a FPI apparatus is shown in Figure 2. The light from a laser source is passed though a polarizer to assure that its polarization is vertical (perpendicular to the scattering plane) and then focused onto a sample. The component of the scattered light with horizontal polarization (that is, in the scattering plane) is selected by means of an analyzing polarizer and then, after some optical processing, is passed into a FPI. The interferometer scans the spectrum of the scattered light, which is then detected and analyzed by the photomultiplier tube and photon counting system. For nanoparticles, a confocal FPI is often used.

For a dilute solution of cylindrically symmetric nanoparticles undergoing rotational diffusion, the spectrum of depolarized light measure is proportional to

$$I_{\mathrm{vh}}(\omega) = A\beta^2 \frac{6D_{\mathrm{R}}}{\omega^2 + (6D_{\mathrm{R}})^2} \tag{9}$$

where A is a constant proportional to the nanoparticle concentration, β is the optical anisotropy of the particle, ω is the frequency difference of the scattered light from that of the incident light, and D_{R} is the rotational diffusion coefficient of the symmetry axis of the nanoparticle. The spectrum of scattered light is thus a 'Lorentzian' with a half-width at half-height given by $6D_{\mathrm{R}}$.

As in PCS, we may relate the hydrodynamic quantity, in this case, the rotational diffusion coefficient at infinite dilution, to the particle dimensions. For a spherical particle the Stokes–Einstein–Debye equations relates D_{R} to the particle radius

$$D_{\mathrm{R}} = \frac{k_{\mathrm{B}}T}{8\pi\eta R^3}. \tag{10}$$

As we discussed in the section on PCS above, we may use Eq. (10) for non-spherical particles with the understanding that the radius derived ('rotational hydrodynamic radius') does not correspond to a geometrical radius. Note from Eq. (10) that the rotational diffusion coefficient is proportional to the inverse third power of the particle radius and thus is more sensitive to size than the translational diffusion coefficient (Eq. (4)).

For non-spherical particles, such as rigid rods and ellipsoids of revolution, there are equations relating the infinite dilution translational and rotational diffusion coefficients (and, of course, hydrodynamic radii) and the actual particle dimensions. The best known of these are the Perrin relations for ellipsoids of revolution (Perrin, 1934, 1936). Broersma has derived relations for long rods (Broersma, 1960, 1980) and Garcia de la Torre et al. (Tirado & Garcia de la Torre, 1979, 1980; Tirado et al., 1984; Garcia de la Torre et al., 1984) have derived expressions applicable to shorter rods.

Since ellipsoids of revolution and rods are each characterized by two dimensions, two independent measurements are required to obtain both quantities. Measurements of both D and D_{R} are often used in connection with the theories to obtain both molecular dimensions. We give an example of the application of the Garcia de la Torre et al. relations to the interpretation of PCS and depolarized FPI experiments on a series of oligonucleotides.

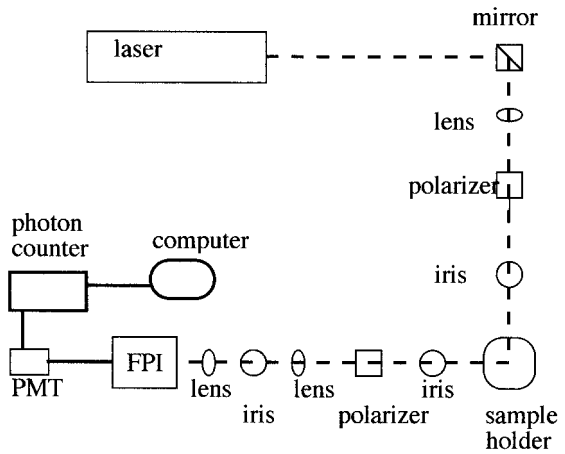

Figure 2. Schematic diagram of a depolarized FPI apparatus.

Both PCS and depolarized FPI have been applied to nanoparticles in liquid dispersions. Depolarized FPI has been less extensively used than PCS. It is relatively more difficult to do than PCS and is not as generally applicable. PCS can usually be used to measure translational diffusion of particles in the range from 1 to 1000 nm, although the technique needs special care at both limits of this range. Common limitations in PCS for small particles in dilute dispersions include weak scattering signals and fast decay of the PCS time correlation function. The weak signal limitation can be overcome in most cases by a variety of methods – more intense laser sources, higher concentrations of nanoparticles, more efficient detectors, etc. Observing the scattering at smaller scattering angle and/or using a more viscous suspending liquid can slow the time decay of the correlation function.

Because of the limited resolution of an FPI, one is often restricted to nanoparticles below about 10 nm in characteristic dimension. For larger particles, usually larger than the upper limit of the nanoparticle size range (about 50 nm), depolarized PCS may often be used (Zero & Pecora, 1982). (The set of depolarized DLS techniques including both depolarized FPI and depolarized PCS is often referred to as DDLS). Nevertheless depolarized FPI is a very powerful technique.

Example – oligonucleotides

To illustrate these techniques, we briefly describe here PCS and depolarized FPI experiments done by Eimer and Pecora (1991) on a series of short oligonucleotides. The oligonucleotides studied were in the B-duplex form – small double helical, rigid – nanoparticles. They are good model systems since they can be made almost monodisperse and thus the complications of polydispersity are minimized. As a first approximation, short double helical oligonucleotides may be modeled as rigid rods.

For rigid rods, the translational and rotational diffusion coefficients of rigid rods of length L and cross-section diameter d may, respectively, be written in the forms

$$D = \left(\frac{k_B T}{3\pi\eta L}\right)(\ln p + \nu) \tag{11}$$

and

$$D_R = \left(\frac{3k_B T}{\pi\eta L^3}\right)(\ln p + \delta) \tag{12}$$

where $p = L/d$ and ν and δ are called 'end-effect' corrections.

The differences between various theories for the diffusion coefficients of rods are in the end effect corrections ν and δ. Tirado, Lopez Martinez and Garcia de la Torre (Tirado & Garcia de la Torre, 1979, 1980; Tirado et al., 1984; Garcia de la Torre et al., 1984) have given expressions for these corrections. A polynomial approximation to their numerical results has been obtained for the range $2 < p < 30$:

$$\nu = 0.312 + 0.565p^{-1} - 0.100p^{-2} \tag{13}$$

and

$$\delta = -0.662 + 0.917p^{-1} - 0.050p^{-2} \tag{14}$$

A technique for obtaining hydrodynamic dimensions of rodlike molecules using Eqs. (11)–(14) has been given by Garcia de la Torre, Lopez Martinez, and Tirado (Garcia de la Torre et al., 1984). They first compute a function $f(p)$ defined as

$$f(p) = \left(\frac{9\pi\eta}{k_B T}\right)^{2/3} \frac{D}{D_R^{1/3}} = \frac{\ln p + \nu}{(\ln p + \delta)^{1/3}} \tag{15}$$

The procedure is then to make a theoretical plot of $f(p)$ versus p based on Eqs. (13) and (14); obtain a value of $f(p)$ from measurement of D and D_R; use the theoretical plot to obtain the experimental p, and then use this p and the experimental diffusion coefficients to obtain L (and d) from either (or both) Eqs. (11) and (12).

Eimer and Pecora (1991) performed PCS and depolarized FPI experiments on oligonuleotides 8, 12 and 20 base pairs in length in a water-based phosphate buffer at pH = 7. Measurements were done at various temperatures and then corrected to 20°C. Figures 3 and 4 show, respectively, translational and rotational diffusion coefficients measured for these oligonucleotides as functions of oligonucleotide concentration. The D_0 and k_D from the straight line fits from Figure 3 and the D_R from Figure 4 (which are constant in the lower concentration range studied) are listed in Table 1.

Using these D_0 and D_R values and the procedure of Garcia de la Torre, Lopez Martinez and Tirado to model the results, they obtain the lengths and diameters given in the table. We note that to within the error of the experiment and analysis (about ± 0.15 nm) the diameters of this homologous series are the same. This is taken to indicate that the theoretical relations used are consistent. It also indicates that the effective hydrodynamic cross-section rod diameter of DNA is less than

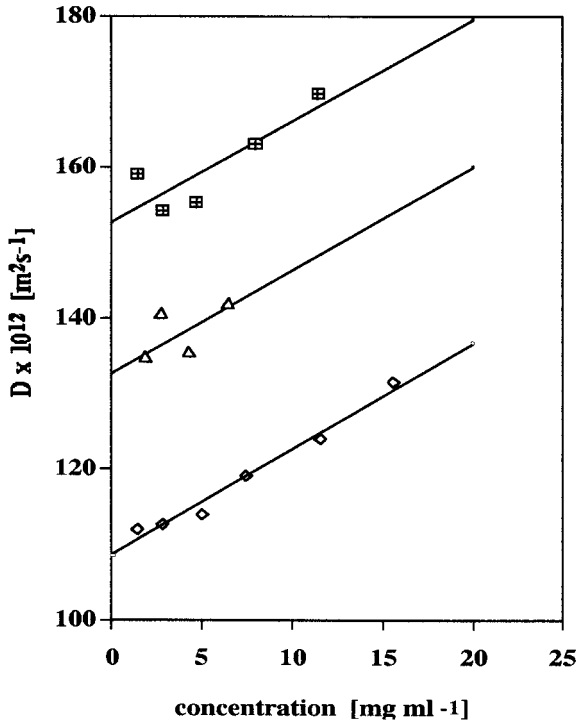

Figure 3. Translational diffusion coefficients for the oligonucleotides versus concentration corrected to 20°C. The temperature range of the measurements was 10–50°C. From top to bottom: 8-mer, 12-mer, 20-mer.

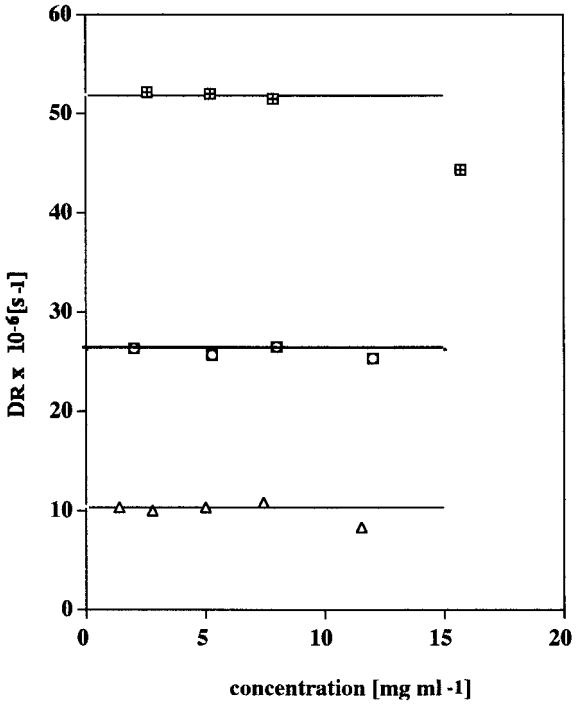

Figure 4. Rotational diffusion coefficients versus concentration corrected to 20°C for the three oligonucleotides. From top to bottom: 8-mer, 12-mer, 20-mer. The highest concentration point for the 8-mer is indicative of aggregation.

Table 1. Diffusion coefficients of oligonucleotides at 20°C and derived dimensions

D_0 (10^{-12} m^2 s^{-1})	k_D (10^{-3} ml mg^{-1})	D_R (10^6 s^{-1})	$f(p)$	p	L (nm)	d (Å)	
8-mer	152.6	8.5	51.8	1.50	1.43	2.86	20.0
12-mer	134.1	8.0	26.1	1.63	2.10	4.21	20.1
20-mer	108.6	12.9	10.3	1.83	3.59	6.88	19.2

has normally been assumed (2.4–2.6 nm). The larger hydrodynamic cross-section diameter relative to the X-ray dimensions found in the solid were attributed to water of hydration that was carried by the DNA as it moved through the solution. These larger values, however, were measured on longer fragments than were used by Eimer and Pecora. The longer fragments have diffusion coefficients that are less sensitive to the diameter. The longer ones might also exhibit complications from flexibility.

The measurements of Eimer and Pecora were done at relatively high ionic strengths, and dilute concentrations. One complication that occurs in solutions of charged molecules such as the oligonucleotides (which ionize at pH values near neutral) is that even at relatively dilute concentrations, the oligonucleotides can interact through long range Coulomb forces. At high ionic strengths, obtained by adding a salt such as NaCl to the solution, these long range forces are screened by the small ions and the various expressions given for the diffusion coefficients described above apply. However, at low ionic strengths these long range interactions can become important and strongly affect the diffusion coefficients (Liu et al., 1998). Another

complication that occurs at low ionic strengths is the appearance of a 'slow mode' in the PCS time correlation function (Skibinska et al., 1999). The origin of the slow mode is controversial, but it appears to be due to long range correlation between oligonucleotides.

Since rotational and translational diffusion coefficients are very sensitive to molecular dimensions, the method may also be used, often in conjunction with some of the modeling techniques for complex shapes described in the next section, to monitor conformational changes such as the *B* to *Z* transition in oligonucleotides (Haber-Pohlmeier & Eimer, 1993), and aggregation and self-assembly processes in oligonucleotides, proteins and other nanoparticles (Michielsen & Pecora, 1981; Patkowski et al., 1990; 1991; Eimer & Dorfmüller, 1992; Eimer et al., 1993).

Nanoparticles with complex shapes

A more powerful procedure than using simple shapes such as spheres, rods and ellipsoids of revolution to model nanoparticles is to use the actual shape of rigid non-spherical particles at the atomic or monomer level and then to compute the diffusion coefficients (or hydrodynamic radii) for this usually complex structure using sophisticated algorithms (Teller et al., 1979; Garcia de la Torre & Bloomfield, 1981; Garcia de la Torre & Rodes, 1983; Garcia de la Torre et al., 1994; Venable & Pastor, 1988; Byron, 1997; Hellweg et al., 1997; Banochowicz et al., 2000). The theoretical result is then compared to experimentally determined diffusion coefficients and hydrodynamic radii. If several structural models of the nanoparticle are possible, then this approach may often be used to distinguish between them. This procedure is often used for biologically important nanoparticles (proteins, nucleic acids, etc.) in which it is desirable to determine details of the particle structure.

Conclusion

DLS is the method of choice for studying nanoparticles in liquids. It will play an even more important role in coming years as the experimental techniques are further refined and the range of application and ease of use are extended. Powerful DLS techniques not described above may also be applied to specialized situations. For instance, electrophoretic light scattering allows the simultaneous measurement of electrophoretic mobilities and translational diffusion coefficients (Ware et al., 1983). Diffusing wave spectroscopy is applicable to dispersions in which the scattering is so intense and multiple scattering is so important that photons 'diffuse' through the liquid (Durian et al., 1991). Two color and 3D PCS are also applicable to strongly scattering systems. These are cross-correlation techniques that can be utilized to measure the single scattered light in the presence of multiply scattered light (Overbeck & Sinn, 1999). Another exciting development is the extension of the PCS techniques developed for light sources in or near the visible region to the X-ray region. This technique, usually referred to as XPCS, is now under rapid development (Dierker et al., 1995; Thurn-Albrecht et al., 1999).

References

Aragon S.R. & R. Pecora, 1975. Biopolymers 14, 119.

Banachowicz E., J. Gapinski & A. Patkowski, 2000. Biophys. J. 78, 70.

Berne B.J. & R. Pecora, 2000. Dynamic Light Scattering. Dover Publications, New York.

Broersma S., 1960. J. Chem. Phys. 32, 1626, 1632; ibid. 1980. 74, 6889.

Brown W., ed., 1993. Dynamic Light Scattering: The Method and Some Applications. Clarendon Press, Oxford.

Bu Z., P.S. Russo, D.L. Tipton & I.I. Negulescu, 1994. Macromolecules 27, 6871.

Byron O., 1997. Biophys. J. 72, 408.

Camins B. & P.S. Russo, 1994. Langmuir 10, 4053.

Chu B., 1991. Laser Light Scattering, 2nd edn. Academic Press, New York.

Chu B. & T. Liu, 2000. J. Nanopart. Res. 2, 29.

Dierker S. et al., 1995. Phys. Rev. Lett. 75, 449.

Durian D.J., D.A. Weitz & D.J. Pine, 1991. Science 252, 686.

Eden D. & J.G. Elias, 1983. In: B.E. Dahneke, ed. Measurement of Suspended Particles by Quasi-Elastic Light Scattering. Wiley-Interscience, New York.

Eimer W. & R. Pecora, 1991. J. Chem. Phys. 94, 2324.

Eimer W. & Th. Dorfmüller, 1992. J. Phys. Chem. 96, 6790.

Eimer W., M. Niermann, M.A. Eppe & B.M. Jockusch, 1993. J. Mol. Biol. 229, 146.

Flamberg A. & R. Pecora, 1984. J. Phys. Chem. 88, 3026.

Garcia de la Torre J., M.C. Lopez Martinez & M.M. Tirado, 1984. Biopolymers 23, 611.

Garcia de la Torre J. & V. Bloomfield, 1981. Q. Rev. Biophys. 14, 81.

Garcia de la Torre J., S. Navarro & M.C. Lopez-Martinez, 1994. Biophys. J. 66, 1573.

Garcia de la Torre J. & J. Rodes, 1983. J. Chem. Phys. 79, 2454.

Graf C., W. Schaertl, M. Maskos & M. Schmidt, 2000. J. Chem. Phys. 112, 3031.

Haber-Pohlmeier S. & W. Eimer, 1993. J. Phys. Chem. 97, 3095.
Hellweg T., W. Eimer, E. Krahn, K. Schneider & A. Müller, 1997. Biochem. Biophys. Acta. 337, 311.
Kaszuba M., 1999. J. Nanopart. Res. 1, 405.
Lakowicz J.R., 1983. Principles of Fluorescence Spectroscopy. Plenum, New York.
Liu H., L. Skibinska, J. Gapinski, A. Patkowski, E.W. Fischer & R. Pecora, 1998. J. Chem. Phys. 109, 7556.
Michielsen S. & R. Pecora, 1981. Biochemistry 20, 6994.
Overbeck E. & Chr. Sinn, 1999. J. Mod. Optics 46, 303.
Patkowski A., W. Eimer & Th. Dorfmüller, 1990. Biopolymers 30, 93.
Patkowski A., W. Eimer, J. Seils, G. Schneider, B.M. Jockusch & Th. Dorfmüller, 1991. Biopolymers, 30, 1281.
Pecora R., ed., 1985. Dynamic Light Scattering: Applications of Photon Correlation Spectroscopy. Plenum, New York.
Perrin F., 1934. J. Phys. Rad. 5, 497; ibid. 1936. 7, 1.
Piazza R. & V. Gegiorgio, 1992. Physica A 182, 576.
Piazza R., J. Stavans, T. Bellini & V. Degiorgio, 1989. Opt. Commun. 73, 263.
Provencher S.W., 1982. Comput. Phys. Comm. 27, 213, 239.
Pusey P.N., R.J.A. Tough, 1985. In: R. Pecora, ed. Dynamic Light Scattering: Applications of Photon Correlation Spectroscopy. Plenum, New York.
Righini R., 1993. Science 262, 1386.
Schmitz K.S., 1990. An Introduction to Dynamic Light Scattering by Macromolecules. Academic Press, San Diego.
Schrof W., J. Klingler, W. Heckmann & D. Horn, 1998. Colloid. Polym. Sci. 276, 577.
Skibinska L., H. Liu, J. Gapinski, A. Patkowski, E.W. Fischer & R. Pecora, 1999. J. Chem. Phys. 110, 1794.
Startchev K., J. Zhang & C. Buffle, 1998. J. Coll. Interface Sci. 12.203, 189.
Teller D.C., E. Swanson & C. de Haen, 1979. Adv. Enzymol. 61, 103.
Thurn-Albrecht T. et al., 1999. Phys. Rev. E 59, 642.
Tirado M.M. & J. Garcia de la Torre, 1979. J. Chem. Phys. 71, 2581; ibid. 1980. 73, 1986.
Tirado M.M., M.C. Lopez Martinez & J. Garcia de la Torre, 1984. J. Chem. Phys. 81, 2047.
Venable R.M. & R.W. Pastor, 1988. Biopolymers 27, 1001.
Vo-Dinh T., G.D. Griffin, J.P. Alarie, B. Cullum, B. Sumpter & D. Noid, 2000. J. Nanopart. Res. 2, 17.
Ware B.R., D. Cyr, S. Gorti & F. Lanni, 1983. In: B.E.Dahneke, ed. Measurement of Suspended Particles by Quasi-Elastic Light Scattering. Wiley-Interscience, New York.
Wiese H. & D. Horn, 1991. J. Chem. Phys. 94, 6329.
Zero K.M. & R. Pecora, 1982. Macromolecules 15, 87.